

1/f Flux Noise in Josephson Phase Qubits

Radoslaw C. Bialczak,¹ R. McDermott,² M. Ansmann,¹ M. Hofheinz,¹ N. Katz,¹ Erik Lucero,¹ Matthew Neeley,¹
A. D. O'Connell,¹ H. Wang,¹ A. N. Cleland,¹ and John M. Martinis^{1,*}

¹*Department of Physics, University of California, Santa Barbara, California 93106, USA*

²*Department of Physics, University of Wisconsin–Madison, Madison, Wisconsin 53706, USA*

(Received 11 August 2007; published 2 November 2007)

We present a new method to measure $1/f$ noise in Josephson quantum bits (qubits) that yields low-frequency spectra below 1 Hz. A comparison of the noise taken at positive and negative bias of a phase qubit shows the dominant noise source to be flux noise and not junction critical-current noise, with a magnitude similar to that measured previously in other systems. Theoretical calculations show that the level of flux noise is not compatible with the standard model of noise from two-level state defects in the surface oxides of the films.

DOI: [10.1103/PhysRevLett.99.187006](https://doi.org/10.1103/PhysRevLett.99.187006)

PACS numbers: 74.40.+k, 03.67.-a, 85.25.-j

Superconducting integrated circuits are a leading candidate for scalable quantum information processing (QIP) [1]. Quantum bits (qubits) based on Josephson junctions have already achieved several key milestones, including single and coupled qubit state tomography [2,3]. Moreover, the dominant mechanism for energy relaxation is becoming understood [4], and steady improvements can be expected in the coming years. However, to realize the full potential of Josephson junctions for QIP, it will be necessary to extend qubit dephasing times. Present dephasing times are in the 100s of ns range; the short coherence places a strict limit on the number of gate operations that can be implemented and represents a significant obstacle to scaling up. Dephasing is produced by low-frequency fluctuations in the qubit energy. In the case of the Josephson flux qubit and the flux-biased Josephson phase qubit, these fluctuations are believed to arise from a magnetic flux noise applied to the qubit loop, with a spectral density that scales inversely with frequency ($1/f$). Moreover, the magnitude of the flux noise inferred from qubit Ramsey fringe experiments is of the order of several $\mu\Phi_0/\sqrt{\text{Hz}}$ for both three-junction flux qubits and phase qubits, despite a difference in loop inductance of almost 2 orders of magnitude [5].

Low-frequency noise in superconducting circuits has been studied for decades in the context of amplifiers based on the superconducting quantum interference devices (SQUIDs) [6,7]. More than 20 years ago in a series of experiments on SQUIDs cooled to milli-Kelvin temperatures, researchers found that the devices displayed a flux noise with a power spectrum that scaled like $1/f^\alpha$ at low frequencies, where α lies in the range from 0.6 to 1. The magnitude of the noise was seen to be only weakly dependent on a wide range of device parameters such as SQUID loop inductance, geometry, material, etc., with a canonical value at 1 Hz of about $2\mu\Phi_0/\sqrt{\text{Hz}}$. The origin of the excess low-temperature flux noise in these experiments was never understood, and the issue has lain dormant for

almost two decades. Now it seems clear that the excess low-temperature noise of these SQUIDs is intimately connected to the measured dephasing times of superconducting qubits [5,8,9].

In this Letter we present the results of a novel measurement in a Josephson phase qubit that uses the resonant response of the qubit to directly measure the spectrum of low-frequency noise. This general method can be used for any qubit system. By alternating the sense of the qubit bias, we show that the noise is predominantly fluxlike, as opposed to a critical-current noise. This experiment is the first to directly connect flux noise in superconducting qubits to previous measurements in SQUID devices. Additionally, we present the results of calculations of flux noise from paramagnetic defects in the native oxides of the superconductors, and show that the measured flux noise is not compatible with the standard model of two-level state (TLS) defects.

A photomicrograph of our device is shown in Fig. 1; a more detailed discussion of its operation is given elsewhere [10]. A current bias $I = \Phi/L$ is applied to the Josephson junction via a flux Φ threading an inductor L placed across the junction. The bias current is set slightly below the critical current of the junction I_0 so that the system can be well modeled by a cubic potential (see inset). The two lowest quantum states in this potential well are labeled as qubit states $|0\rangle$ and $|1\rangle$, and have an energy difference E_{10} that can be tuned with bias. Transitions between $|0\rangle$ and $|1\rangle$ are driven by applying microwaves at a frequency $\omega_{10}/2\pi = E_{10}/h \sim 6$ GHz. The qubit state is measured by applying a fast bias pulse to lower the potential barrier, forcing only the $|1\rangle$ state to tunnel out of the well [11].

The transition frequency ω_{10} is given by

$$\omega_{10} \simeq \omega_{p0}(1 - |I|/I_0)^{1/4}, \quad (1)$$

where $\omega_{p0} = 2^{1/4}(2\pi I_0/C\Phi_0)^{1/2}$. Low-frequency fluctuations in the current bias I and critical current I_0 produce fluctuations in the transition frequency primarily from the

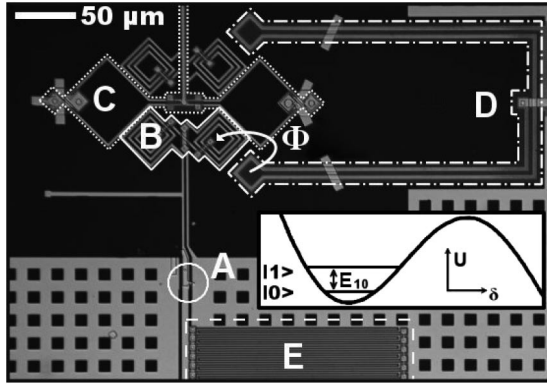


FIG. 1. Photomicrograph of Al-based qubit fabricated on a sapphire substrate using a SiN_x dielectric for crossover wiring. (a) Josephson junction with area $A_J \sim 2 \mu\text{m}^2$ and critical current $I_0 = 1.9 \mu\text{A}$. (b) Qubit inductor with inductance $L = 800 \text{ pH}$. (c) Readout SQUID. (d) Qubit flux bias. (e) Qubit shunt capacitor with $C = 1 \text{ pF}$. Inset: Qubit potential energy U as a function of the superconducting phase δ across the qubit Josephson junction.

second term. The qubit can be operated at both positive and negative current bias. A positive fluctuation in I_0 gives an increase in ω_{10} at both positive and negative current bias, a symmetric change. A fluctuation in I , however, gives an asymmetric change. Therefore, a spectroscopic measurement of the transition frequency at positive and negative bias currents provides a clear differentiation between these two different noise sources. Moreover, the steep response of the resonance allows for a reasonably sensitive measurement of the fluctuation magnitude.

The experiment is performed by choosing positive and negative current biases close to the critical current, corresponding to flux biases Φ_+ and Φ_- , that have approximately equal transition frequencies. A spectroscopic measurement is then performed by applying a long $2 \mu\text{s}$ microwave pulse and measuring the probability P_1 of the occupation of the $|1\rangle$ state. The amplitude of the microwave excitation is chosen so that $P_1 \lesssim 0.4$ at peak response to prevent significant power broadening of the qubit response. Qubit response curves for positive and negative biases are shown in Figs. 2(a) and 2(c).

As shown by Eq. (1), fluctuations in bias and critical current will cause these resonance curves to shift. The probability P_1 is most sensitive to qubit bias at the half maximum points of the resonance curves, labeled as frequencies ω_L^- , ω_R^- and ω_L^+ , ω_R^+ in Figs. 2(a) and 2(c), respectively. A plot of P_1 versus time is shown for these four frequencies in Figs. 2(b) and 2(d). An anticorrelated change in P_1 within the data pairs (ω_L^-, ω_R^-) and (ω_L^+, ω_R^+) is expected and represents a systematic check of the measurement method. The small deviations from anticorrelation are due to other influences, such as fluctuations of resonant TLS defects [11], which affect the measurement probability pairs in a correlated manner.

The data at ω_L^+ and ω_R^- show symmetric correlation of P_1 with time, as can be seen from the traces in Figs. 2(b) and 2(d). This shows that the dominant low-frequency noise for the qubit is a flux noise. The relation between P_1 and flux is calibrated by measuring P_1 while sweeping the qubit flux bias for each of the four frequencies. The flux noise data measured at ω_L and ω_R are averaged for positive and negative bias, then Fourier transformed, cross-

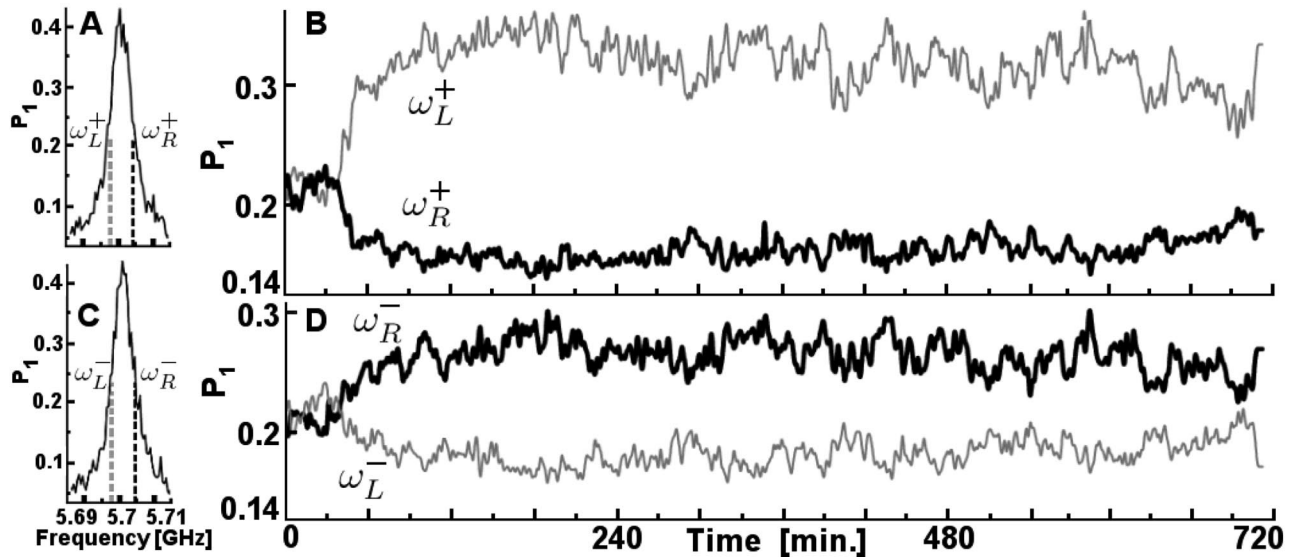


FIG. 2. (a) Qubit response curve for the probability P_1 of the qubit in the $|1\rangle$ state versus microwave excitation frequency at the positive flux bias Φ_+ . (b) The time evolution of P_1 is measured for Φ_+ at the two frequencies ω_L^+ and ω_R^+ , which are shown in (a). (c) and (d) are the same as (a) and (b), respectively, but are for Φ_- . In (b) and (d), data were taken at approximately 800 samples per second. The correlation in ω_L^+ and ω_R^- indicates flux noise.

correlated, and averaged over frequency to obtain the cross-correlated flux noise spectrum plotted in Fig. 3(a). We note that white noise from the measurement process is automatically subtracted in this cross-correlation analysis. The noise has a $1/f^\alpha$ spectrum with $\alpha = 0.95$ and extrapolates to a flux noise at 1 Hz of $4\mu\Phi_0/\sqrt{\text{Hz}}$. This magnitude is comparable with previous measurements of $1/f$ flux noise in superconducting devices [6,7].

In Fig. 3(b) we plot the correlation amplitude and phase angle of the cross-correlated flux noise spectrum. The correlation angle of zero indicates asymmetric (fluxlike) noise. At the lowest frequencies, the contribution from measurement noise is small. The saturation of the correlation amplitude at a value slightly less than unity may indicate a small contribution from junction critical-current noise. Taking the contribution from critical-current noise to be $\sim 5\%$, we find $S_{I_0}(1 \text{ Hz}) = 0.05S_\Phi(1 \text{ Hz})/L^2 = 1.4 \times 10^{-12} I_0^2/\text{Hz}$ for our $2 \mu\text{m}^2$ area junction. This value is compatible with previous experiments [7], giving a critical-current noise at 20 mK that is a factor of 36 lower than predicted for 4.2 K [12].

We note that flux noise produces dephasing of the qubit state, as can be measured directly in a Ramsey fringe experiment. The magnitude of our noise is within a factor of 2 of that required to explain our qubit dephasing times of around 200 ns [8].

In what follows, we examine the possibility that the flux noise is due to magnetic TLS defects in the native oxides of the superconducting films, as was recently proposed in Ref. [9]. The standard TLS model [13] describes an ensemble of defects, each with two microscopic configurational states $|L\rangle$ and $|R\rangle$ that have a two-state Hamiltonian with diagonal matrix elements $\pm\Delta/2$ and off-diagonal elements $\Delta_0/2$ due to tunneling. The eigenstates are given

by $|g\rangle = \sin(\theta/2)|L\rangle + \cos(\theta/2)|R\rangle$ and $|e\rangle = \cos(\theta/2)|L\rangle - \sin(\theta/2)|R\rangle$, where $\theta = \arctan(\Delta_0/\Delta)$. The difference in energy of the two states is $E = \sqrt{\Delta^2 + \Delta_0^2}$. The defects are assumed to have a constant distribution of energies Δ , but a log-uniform distribution in Δ_0 because tunneling is exponentially dependent on parameters. Upon changing variables to $(E, \sin\theta)$, the joint distribution is given by $d^2N = \rho dE d\sin\theta / \sin\theta \cos\theta$, where ρ is a materials constant describing the defect density of states. Dipole radiation of the TLS via phonons gives a relaxation rate determined by the matrix element $\sin\theta$, yielding $\Gamma_1 = \Gamma_1^{\max} \sin^2\theta$. The resulting log-uniform distribution of Γ_1 produces a $1/f$ noise spectrum.

To estimate the magnitude of the flux noise from magnetic TLS defects, we consider a TLS magnetic moment equal to the Bohr magneton μ_B , and further assume that fluctuation of the TLS will completely randomize this magnetic moment (we discuss the validity of this assumption below). Following the analysis of Ref. [14], one can show that the low-frequency spectral density of the TLS magnetic moment per unit volume is given by

$$S_m(\omega/2\pi) \simeq 4kT\mu_B^2\rho \int_0^{\Gamma_1^{\max}} \frac{d\Gamma_1}{2\Gamma_1} \frac{2\Gamma_1}{\Gamma_1^2 + \omega^2} \quad (2)$$

$$\simeq \frac{kT\mu_B^2\rho}{\omega/2\pi}. \quad (3)$$

In order to connect the above expression to the measured flux noise, we need to know how each TLS couples magnetically to the SQUID. Analytical expressions for flux noise may be calculated using reciprocity: the magnetic flux from a spin of moment m is given by $(B \cdot m)/I$, where B is the magnetic field at the spin produced by a test current I in the SQUID loop. We consider two idealized SQUID geometries that are amenable to analytical treatment. First, we consider a thin wire of diameter D in a circular loop of radius R with $R \gg D$. We find that the mean-square flux induced in the SQUID by the TLS defects is given by

$$\langle \Phi^2 \rangle = \frac{2\mu_0^2}{3} \mu_B^2 \sigma \frac{R}{D}, \quad (4)$$

where σ is the density of TLS surface defects on the superconducting wire. A factor $1/3$ arises from a random angular distribution of the TLS magnetic moments. For the more realistic geometry of a thin-film superconductor of width W and thickness b in a circular loop of radius R with $R \gg W \gg b$, the surface currents $J(x)$ at position $-W/2 + \lambda < x < W/2 - \lambda$ are proportional to $[1 - (2x/W)^2]^{-1/2}$, where λ is the penetration depth [15]. The currents fall away exponentially to zero at the edges $\pm W/2$. With the surface magnetic field being proportional to the surface current density, the mean-square flux coupled to the SQUID is calculated as follows:

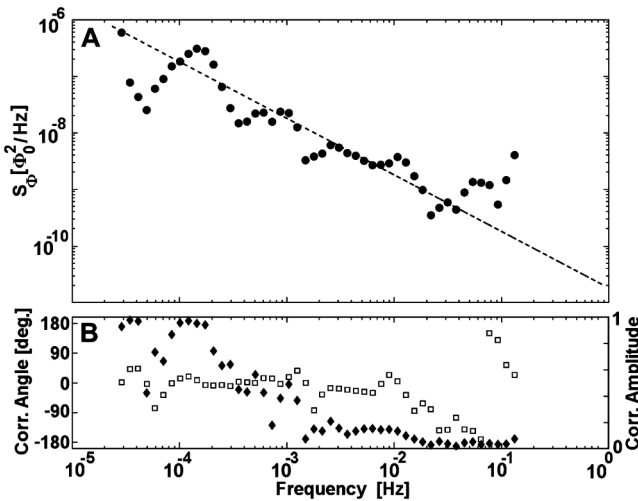


FIG. 3. (a) Cross-correlated noise power spectrum of data taken from Figs. 2(b) and 2(d). The line for an ideal $1/f$ spectrum is shown for reference. (b) Correlation amplitude (diamonds) and phase angle (squares) of cross-correlated data in (a).

$$\langle \Phi^2 \rangle = (\pi/6) \mu_0^2 \mu_B^2 \sigma R \frac{\int dx J^2(x)}{[\int dx J(x)]^2} \quad (5)$$

$$\simeq \frac{2\mu_0^2}{3} \mu_B^2 \sigma \frac{R}{W} \left[\frac{\ln(2bW/\lambda^2)}{2\pi} + 0.27 \right]. \quad (6)$$

The logarithmic term changes the prediction of Eq. (4) by a factor ~ 1.8 , with a reasonable fraction of the noise arising from fluctuators within a few penetration depths near the edges of the film.

The major geometric dependence of the noise comes from the ratio R/W , the loop radius to width, with only a logarithmic dependence on the overall scale [16]. This feature of the model is compatible with the observation that the flux noise of μm -sized flux qubits is similar to that found for our 200 μm scale qubit, as the geometric ratio R/W is similar for these devices.

The critical parameter determining the magnitude of the noise is the surface density of defect states $\sigma = \rho t$, where t is the thickness of the surface oxide on the superconducting film. The TLS defect density in amorphous oxide films can be extracted from measurements of the loss tangent of large-area tunnel junctions [4]. It is found that this defect density is compatible with bulk values obtained for a wide variety of amorphous oxides. We therefore take as an estimate of the TLS surface density [4] $\rho t = 1.0/\mu\text{m}^2(\text{hGHz})$, twice that measured in tunnel junctions, to account for the thicker surface oxide $t \sim 2$ nm. To calculate the spectral density of the flux noise, we substitute $S_m t$ for $\mu_B^2 \sigma$ in Eq. (6). Using the parameters $R/W = 10$ and $T = 100$ mK, we compute a flux noise spectral density $S_\Phi(1 \text{ Hz}) = 1.1 \times 10^{-3} (\mu\Phi_0)^2/\text{Hz}$, about 4 orders of magnitude smaller than the measured flux noise.

Although we have not explicitly considered the noise contribution from other surfaces away from the superconductor or dielectrics in crossover wiring, these small volumes cannot compensate for the large discrepancy between the measured and calculated noise. The substrates are not likely candidates since they are typically crystalline and, therefore, have very low defect densities. In addition, defects at a Si/SiO_x interface cannot account for the measured noise since our devices were made on sapphire substrates.

Moreover, we note that the assumption that TLS fluctuation randomizes the defect magnetic moment is highly questionable because TLS defects in typical oxides are not considered to be magnetic. The above density of magnetic defect states is probably a gross overestimate, further exacerbating the discrepancy between the measured flux noise and the noise calculated from TLS defect states.

If spin noise is responsible for flux noise, we conclude that it must arise from a surface defect mechanism that is very different from that described by the standard TLS model, as it must have a defect/atomic-bond ratio that is about 10^4 times larger than for bulk TLS defects. Such a

model would predict that specific heat measurements for amorphous materials would be dominated by surface states once the thickness of structures is less than about 1–10 μm . Koch *et al.* have suggested [9] surface electronic states as a possible candidate; unfortunately, the density of these defects has been estimated only at room temperature. A possible new mechanism has been proposed based on tunneling of conduction electrons into surface states [17].

In conclusion, we have demonstrated a new measurement of $1/f$ flux noise in superconducting qubits, which allows us to distinguish between flux and critical-current fluctuations. The magnitude of the measured noise is in good agreement with previous experiments, even though device parameters greatly differ. We have also theoretically considered a spin-noise mechanism arising from fluctuating TLS. With the predicted magnitude in disagreement by over 4 orders of magnitude, we conclude that any model for spin noise must arise from a new mechanism based on a high density of defects.

We thank C. Yu, L. Faoro, and L. Ioffe for discussions on magnetic TLS defects. Devices were made at the UCSB and Cornell NanoScale Facilities, a part of the NSF-funded National Nanotechnology Infrastructure Network. This work was supported by Disruptive Technology Office under Grant No. W911NF-04-1-0204 and by NSF under Grant No. CCF-0507227.

*martinis@physics.ucsb.edu

- [1] A. O. Niskanen *et al.*, Science **316**, 723 (2007); D. I. Schuster *et al.*, Nature (London) **445**, 515 (2007); J. H. Plantenberg *et al.*, Nature (London) **447**, 836 (2007); D. Vion *et al.*, Science **296**, 886 (2002).
- [2] M. Steffen *et al.*, Phys. Rev. Lett. **97**, 050502 (2006).
- [3] M. Steffen *et al.*, Science **313**, 1423 (2006).
- [4] J. M. Martinis *et al.*, Phys. Rev. Lett. **95**, 210503 (2005).
- [5] F. Yoshihara *et al.*, Phys. Rev. Lett. **97**, 167001 (2006).
- [6] R. H. Koch *et al.*, J. Low Temp. Phys. **51**, 207 (1983).
- [7] C. Wellstood *et al.*, Appl. Phys. Lett. **50**, 772 (1987); Ph.D. thesis, University of California Berkeley, 1988.
- [8] J. M. Martinis *et al.*, Phys. Rev. B **67**, 094510 (2003).
- [9] R. H. Koch *et al.*, Phys. Rev. Lett. **98**, 267003 (2007).
- [10] N. Katz *et al.*, Science **312**, 1498 (2006).
- [11] K. B. Cooper *et al.*, Phys. Rev. Lett. **93**, 180401 (2004).
- [12] B. Savo *et al.*, Appl. Phys. Lett. **50**, 1757 (1987).
- [13] S. Hunklinger and A. K. Raychaudhuri, Prog. Low Temp. Phys. **9**, 265 (1986); *Amorphous Solids: Low-Temperature Properties*, edited by W. A. Phillips (Springer, Berlin, 1981).
- [14] A. Shnirman *et al.*, Phys. Rev. Lett. **94**, 127002 (2005).
- [15] T. Van Duzer and C. W. Turner, *Principles of Superconductive Devices and Circuits* (Prentice-Hall, Englewood Cliffs, NJ, 1998).
- [16] This result scales with size differently than numerically computed in Ref. [9].
- [17] L. Faoro and L. B. Ioffe (private communication).